Analytical Perspective for Bound States in the Continuum in Photonic Crystal Slabs

Yi Yang,[1] Chao Peng,[1,*] Yong Liang,[2] Zhengbin Li,[1] and Susumu Noda[2]

[1]*State Key Laboratory of Advanced Optical Communication Systems and Networks, Department of Electronics,*
Peking University, Beijing 100871, China
[2]*Department of Electronic Science and Engineering, Kyoto University, Kyoto-Daigaku-Katsura,*
Nishikyo-ku, Kyoto 615-8510, Japan

We investigate the formation of photonic bound states in the continuum (BICs) in photonic crystal slabs from an analytical perspective. Unlike the stationary at-Γ BICs which originate from the geometric symmetry, the tunable off-Γ BICs are due to the weighted destructive via the continuum interference in the vicinity of accidental symmetry when the majority of the radiation is precanceled. The symmetric compatible nature of the off-Γ BICs leads to a trapping of light that can be tuned through continuously varying the wave vector. With the analytical approach, we explain a reported experiment and predict the existence of a new BIC at an unrevealed symmetry.

The localization of waves has always been more difficult to manipulate than their propagation. It is well known that an electromagnetic wave of a specific frequency can be trapped by structures such as photonic [1–3] and plasmonic [4] nanocavities, in which outgoing waves are completely forbidden. However, it has been demonstrated that perfect light confinement can still be achieved even with allowed outgoing waves, because of a particular type of localized state: a bound state in the continuum (BIC). Historically, von Neumann and Wigner [5] first proposed that a BIC can be explicitly constructed in a quantum system when the wave function exhibits weakly damped oscillations. Furthermore, the occurrence of BICs was interpreted as the interference of resonances in direct and via the continuum channels [6,7]. It is a very general effect that is important in many areas of physics, including photonics [8–11], quantum [12–16], aquatic, and acoustic waves [17,18], etc. Although some artificially designed potentials cannot be readily realized in an electronic quantum system, similar phenomena may be more easily implemented optically under Maxwell's theory. Recently, BICs have been demonstrated in photonic crystal (PC) slabs [19], in which periodic geometry leads to BICs at Γ on photonic band structures that are analogous to electron band structures in solids.

In many reported cases, BICs are decoupled from continuum states because geometric symmetry forbids coupling to any outgoing wave, i.e., symmetry incompatibility that leads to stationary BICs, namely, fixed BICs at the Γ point. Very recently, another type of BIC was reported in PC slabs on TM-like bands [20,21] at some seemingly unremarkable wave vectors without symmetry incompatibility, giving rise to a tunable trapping of light. This disappearance of leakage was primarily attributed to the destructive interference among several leakage channels, but the underlying physics remains unrevealed.

For a general quantum system, a theory regarding BICs was developed by Feshbach, Friedrich, and Wintgen [6,7] many years ago. It describes two interfering resonances caused by the coupling in closed and open channels. Similar phenomena also occur in a PC slab system in which several guided mode resonances interfere. These resonances are coupled to each other through in-plane Bloch waves (closed channels) or leaky waves (open channels) and form the BICs. Recently, we proposed a coupled-wave theory (CWT) [22–24] for analyzing the guided mode resonance in two-dimensional PC slabs. The CWT depicts the analogous physics in a photonic system in great detail, as did Feshbach's theory for a quantum system. In this Letter, we present a more comprehensive understanding of BICs in PC slabs based on the analytical CWT of PC modes in the continuum.

A tunable BIC has been observed in the structure illustrated in Fig. 1(a) [20] and we focus on this structure for consistency. Assuming the TE-TM coupling is much weaker than their own internal coupling, the TM-like electromagnetic field is given by (H_x, H_y, E_z). For a macroscopic PC slab, assuming that the area in the **xy** plane is infinite, we have $H_i(z) = H_{i,0,0} + \sum_{m \neq 0, n \neq 0} H_{i,m,n}(z) e^{-im\beta_0 x - in\beta_0 y}$, where $\beta_0 = 2\pi/a$. Moreover, within the PC slab ($|z| < d$), $1/\varepsilon(r)$ can be expanded with the Fourier transform: $1/\varepsilon(r) = \kappa_a + \sum \kappa_{mn} e^{-im\beta_0 x - in\beta_0 y}$, where $\kappa_a = f(1/\varepsilon_l) + (1 - f)(1/\varepsilon_{sn})$ (f is the filling factor). Outside the PC slab ($|z| > d$), $1/\varepsilon(r) = 1/\varepsilon_l \triangleq \kappa_b$. The coupling equations of closed and open channels can be obtained from Maxwell's equations, as follows for the **x** direction:

$$\left(\kappa_a\frac{\partial^2}{\partial z^2} + \delta(|d|)\Delta\kappa\frac{\partial}{\partial z} + k_0^2 - \kappa_a n_y^2\beta_0^2\right)H_{x,m,n} + \kappa_a m_x n_y \beta_0^2 H_{y,m,n}$$

$$= \sum_{\substack{m'\neq m, n'\neq n \\ n-n',}} \kappa_{m-m'} \left[\left(-\frac{\partial^2}{\partial z^2} + \delta(|d|)\frac{\partial}{\partial z} + n_y n'_y\beta_0^2\right)H_{x,m',n'} - m'_x n_y \beta_0^2 H_{y,m',n'}\right], \quad (1)$$

where $\Delta\kappa \triangleq \kappa_b - \kappa_a$, $\delta(|d|) \triangleq \delta(z-d) - \delta(z+d)$ and (m_x, n_y) follow the same notations as that used in our previous work [23]. Because of symmetry, the equation for the **y** direction can be readily obtained from Eq. (1) by switching $H_{x,m,n}$, $H_{x,m',n'}$, m_x, and m'_x with $H_{y,m,n}$, $H_{y,m',n'}$, n_y, and n'_y, respectively. In the **z** direction, the transverse wave condition of the **H** components yields

$$\sum_{\substack{m',n' \\ n-n',}} \kappa_{m-m'}\frac{\partial}{\partial z}(m_x H_{x,m',n'} + n_y H_{y,m',n'}) = 0. \quad (2)$$

Because the TM-like modes involve a longitudinal electric field, two effects influence the coupling strength between individual channels: the in-plane coupling caused by the permittivity periodicity and the surface coupling caused by the discontinuities at dielectric interfaces. Essentially different from TE-like modes, the $\delta(|d|)$ part of the operator in Eq. (1) depicts the unique surface coupling existing in TM-like modes only [26]. The remainder of the operator represents the conventional in-plane coupling for both TE and TM-like modes [26,27]. Equation (1) is analogous to Eq. (1) in Friedrich's work for a quantum system that describes the interference of several closed channels with one or more open channel(s) [7].
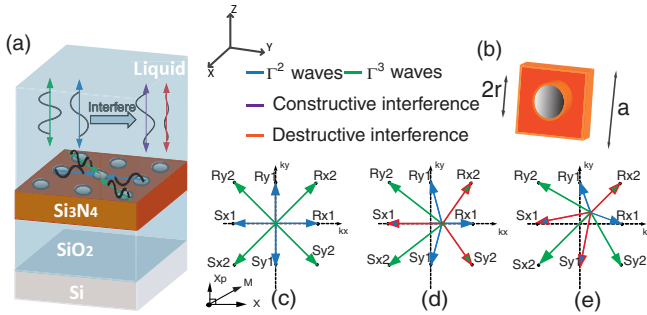

FIG. 1 (color online). (a) Structure: liquid ($\varepsilon_l = 2.11$), Si$_3$N$_4$ PC slab ($\varepsilon_{sn} = 4.08$), silica cladding ($\varepsilon_{so} = 2.13$), and Si substrate. Setting $\varepsilon_l \simeq \varepsilon_{so}$ ensures mirror-flip symmetry [20]. The silica and liquid layers are sufficiently thick to be assumed as infinite. (b) Basic lattice: thickness $2d = 180$ nm, periodicity $a = 336$ nm, hole diameter $2r = 160$ nm. (c),(d),(e) Phase matching conditions: (c) Γ point; (d) $k = 0.25$ in the $\Gamma - X$ direction; (e) $k = \sqrt{2}/6$ in the $\Gamma - M$ direction. Red arrows indicate extra degenerate wave vectors. For square lattice, the Γ^1, Γ^2, and Γ^3 points are defined as wave vectors with lengths of 0, $2\pi/a$, and $2\sqrt{2}\pi/a$, respectively [25].

The guided resonance depends on the phase matching between the guided mode (β) and a given (m, n) order of the Bloch mode ($\beta_{mn} = m\beta_0\hat{x} + n\beta_0\hat{y}$), with $\beta = |\beta_{mn}|$. At the Γ^2 point, with the phase matching given by $\beta = \beta_0$, all Bloch waves except $H_{0,0}$ are confined within the slab. In Fig. 1(c), owing to the symmetry of a square lattice, four wave vectors $\mathbf{V} = \{R_{x1}, S_{x1}, R_{y1}, S_{y1}\}$ can be treated as uncoupled closed channels. The coupling between closed channels can be realized via in-plane waves (through $H_{m,n}$), or via the continuum (through $H_{0,0}$). Thus we have an eigenvalue problem,

$$(\mathbf{k} - \mathbf{k}_{0;mn})\mathbf{V} = \left(\sum_{\substack{m,n;m',n' \\ n-n',}} \langle H_{i,m,n}|\kappa_{m-m'}|H_{i,m',n'}\rangle\right.$$
$$\left. + \sum_{m,n}\langle H_{i,m,n}|\kappa_{m,n}|H_{i,0,0}\rangle\right)\mathbf{V}, \quad (3)$$

where $i = x, y$. Using the approach similar to that for TE-like modes [22], all terms in Eq. (3) can be solved analytically and the complex frequencies are obtained as eigenvalues. Moreover, the leaky wave (open channel) can be calculated in terms of the closed channels,

$$H_{i,0,0} = \sum_{m,n}\langle G|\kappa_{m,n}\left(\frac{\partial^2}{\partial z^2} - \delta(|d|)\frac{\partial}{\partial z}\right)|H_{i,m,n}\rangle, \quad (4)$$

where $G = [k_0^2 + \delta(|d|)\Delta\kappa(\partial/\partial z) + \kappa_a(\partial^2/\partial z^2)]^{-1}$ is the Green function.

The radiative wave includes the contributions from closed channels with different weights and phases [Fig. 1(a)]. We calculate the band structure (with a wave truncation order [22] of 10 for convergence) near the Γ^2 point where four band-edge modes are identified as TM$_{1-4}$ in Fig. 2(a). Moreover, Q_r of the TM$_1$ mode in the vicinity of Γ^2 is depicted using the CWT [Fig. 2(b)]. Because of the geometric symmetry, all of the coupling coefficients (κ_{mn}) are symmetric at Γ [Fig. 1(c)], which leads to complete destructive interference. For TM-like modes, a partial cancellation occurs between the in-plane and surface coupling. As shown in Fig. 2(c), the strengths of the two coupling mechanisms are comparable in amplitude but opposite in sign, which reduces the overall radiation.

The "perfect symmetry" picture for at-Γ BICs cannot straightforwardly explain the recently reported tunable BICs that occur at seemingly unremarkable k points without symmetry incompatibility. From the analytical perspective of CWT, we found the participation of other orders of Γ
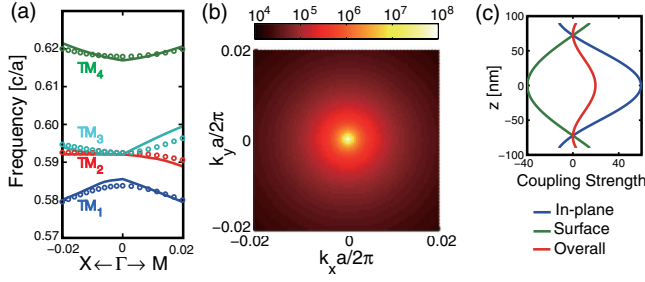
FIG. 2 (color online). (a) Identified TM$_{1-4}$ modes near the Γ^2 point by increasing frequency [25], using both CWT (lines) and finite-difference time domain (FDTD) (dots). (b) CWT-calculated quality factor Q_r of TM$_1$ mode near Γ^2. (c) Precancellation within a closed channel at Γ^2. The coupling strength [22] is defined as $\langle G|\kappa_{m,n}L|H_{i,m,n}\rangle$. For the in-plane coupling, $L = (\partial^2/\partial z^2)$; for the surface coupling, $L = -\delta(|d|)(\partial/\partial z)$.

points may create new symmetry for the formation of tunable BICs.

For the reported tunable BIC at $k \simeq 0.25$ in the $\Gamma - X$ direction [20], the wave vectors of S_{x1}, R_{x2}, and S_{y2} become degenerate and create a new phase matching $\beta = 1.25\beta_0$ via a triangular symmetry [Fig. 1(d)]. As a result, most of the energy coupled to the radiative open channel can be canceled, which forms a $\Gamma - X$ BIC [Fig. 3(a)]. Figure 3(b) shows the radiation ability of the six most significant interfering waves in this case. Among these, S_{x1} has the highest radiation ability while R_{x2} and S_{y2} are comparable. Although R_{y1} and S_{y1} also exhibit considerable contributions; however, the majority of the corresponding radiation cancels with each other because of the symmetry with respect to the **x** axis.

The entire radiation cancellation is demonstrated by mixing all of the participating radiative channels via the mode eigenvectors, as shown in Figs. 3(c) and 3(d). In the **x** direction, all of the radiative waves are canceled because of

symmetry. In contrast, no apparent symmetry holds in the **y** direction. As expected, the radiation projected onto S_{x1} is rather large. The other large component R_{x1} comprises the projection of R_{x2}, S_{y2}, and R_{x1}, in which R_{x2} and S_{y2} dominate because the radiation ability of R_{x1} is rather low [Fig. 3(b)]. Therefore, the accidental degenerate wave vectors S_{x1}, R_{x2}, and S_{y2} contribute dominant radiation, and S_{x1} is in opposite sign with R_{x2} and S_{y2} [Fig. 3(d)]. Hence, by incorporating the radiation from all possible channels, the weighted destructive interference causes the overall radiation to be suppressed (close to 0) as shown in Fig. 3(d).

Interestingly, similar accidental symmetry that may lead to new off-Γ BICs also exists elsewhere. For instance, R_{x2}, S_{x1}, and S_{y2} become degenerate at $k = \sqrt{2}/6$ in the $\Gamma - M$ direction [Fig. 1(e)], forming another triangular symmetry and a new $\Gamma - M$ BIC [Fig. 3(e)]. Fig. 3(f) shows the radiation ability of the five most significant individual waves: S_{x1} and S_{y1} exhibit the highest radiation ability, and the radiation from R_{x2} is also remarkably large. As in the $\Gamma - X$ case, the majority of radiation from R_{x1} and R_{y1} is canceled owing to symmetry [see Fig. 3(g)]. Thus, the degenerate wave vectors S_{x1}, S_{y1}, and R_{x2} contribute dominant radiation.

Choosing the polarizations along the $y = x$ (as x') and $y = -x$ (as y') axes [23] allows for better interpretation of the weighted destructive interference of the $\Gamma - M$ BIC after mixing with the TM$_2$ eigenvectors [Figs. 3(g) and 3(h)]. As previously stated, the radiation in the x' direction remains symmetric and cancels out. In the y' direction, the radiation projected onto S_{x1} and S_{y1} is identical and remarkably large, and their sign is opposite to that of the radiation projected onto R_{x2}. Hence, the weighted destructive interference can be achieved owing to the accidental triangular symmetry, and the overall radiation is suppressed (close to 0).
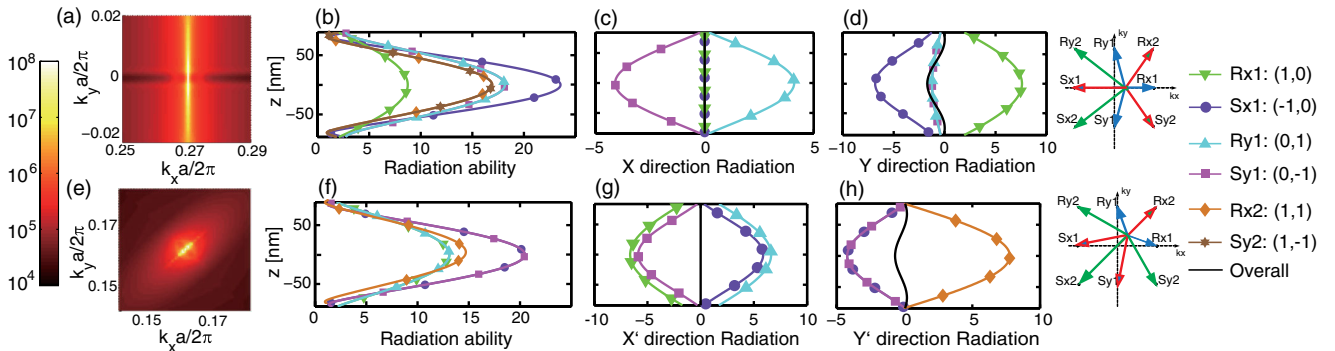

FIG. 3 (color online). CWT-calculated Q_r (a) TM$_1$ mode near $\Gamma - X$ BIC (e) TM$_2$ mode near $\Gamma - M$ BIC. CWT-calculated radiation ability at the symmetry (defined by the modulus of the diffraction into the open channel of individual wave vectors with normalized profiles, i.e., $\|\langle G_{i,-m,-n}H_{i,m,n}\rangle\|$, $i = x, y$) for the (b) $\Gamma - X$ BIC (f) $\Gamma - M$ BIC. Radiation profile decomposition within the slab of (c), (d) TM$_1$ $\Gamma - X$ BIC in the **x** and **y** directions (g),(h) TM$_2$ $\Gamma - M$ BIC in the **x'** ($y = x$) and **y'** ($y = -x$) directions. The radiation profiles are calculated by $P_{m,n}\sum_{m',n'}\langle \mathbf{V}_{TM_{1(2)}}|G_{i,-m',-n'}|H_{i,m',n'}\rangle$, $i = x, y$, where $\mathbf{V}_{TM_{1(2)}}$ is the eigenvector of the $\Gamma - X(M)$ BIC and P_{mn} denotes corresponding projection operators, i.e., $|mn\rangle\langle mn|$.
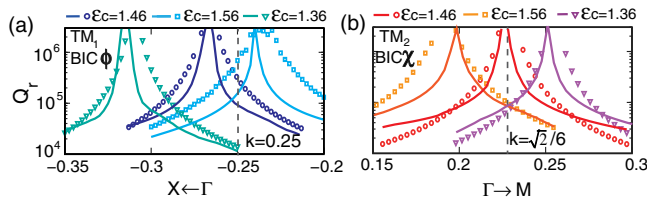
FIG. 4 (color online). Location shift of tunable BICs in the (a) $\Gamma - X$ and (b) $\Gamma - M$ direction using CWT (solid lines) and FDTD (dots). ϵ_c is the cladding permittivity. Dashed lines indicate the exact triangular symmetry [Figs. 1(d) and 1(e)].

FIG. 5 (color online). (a) TM-like and (b) TE-like band structures in the continuum using FDTD. ϕ and χ indicate locations of tunable BICs. Φ and Ξ indicate band gaps formed by triangular symmetry.

The off-Γ BICs do not necessarily occur at the exact accidental symmetry point. Unlike the at-Γ BICs, the off-Γ BICs have different closed-channel weights in their contributions to radiative open channels (determined by κ_{mn}), and hence, a small amount of residual radiation may remain after cancellation at the exact symmetry point. Nevertheless, the interference can be continuously adjusted using the wave vector such that weighted destructive interference always occurs because of the new symmetry, giving rise to a tunable trapping of light. As long as the mirror-flip and inversion symmetry are kept intact [20], tunable BICs can be stably found.

Furthermore, the locations of off-Γ BICs can be shifted by changing various parameters, such as the cladding permittivity ε_c. As shown in Figs. 4(a) and 4(b), the locations of the off-Γ BICs shift away from the Γ point with higher index contrast (i.e., smaller cladding permittivity) and vice versa. When the cladding permittivity varies, the out-of-plane profiles of the individual channels change accordingly, modifying the via the continuum coupling weights, which leads to the location shifts of the tunable BICs.

It should be emphasized that the surface coupling plays an important role in the formation of tunable BICs in TM-like modes. The surface coupling in TM-like modes, unlike that in TE-like modes, precompensates the majority of the large leakage caused by the in-plane coupling in TM-like modes [Fig. 2(c)]. Hence, the sufficiently low radiation ability of the uncoupled closed channels is a prerequisite for the formation of tunable BICs. This criterion also applies for TE-like modes that only possess in-plane coupling, provided that the overall radiation can be effectively suppressed by proper design. For the structure shown in Fig. 1(a), TE-like tunable BICs can hardly be found, as the uncoupled radiation of TE-like modes is too large for via the continuum channels to compensate. We calculate the continuum region for both TE and TM-like modes as shown in Fig. 5. Band gaps Φ and Ξ appear in both TE and TM-like bands, validating the interference by the accidental new phase matchings [Figs. 1(d) and 1(e)]. However, owing to the large radiation ability of the uncoupled channels, TE-like modes can only demonstrate stationary BICs at $k \simeq 0$ with symmetry incompatibility.
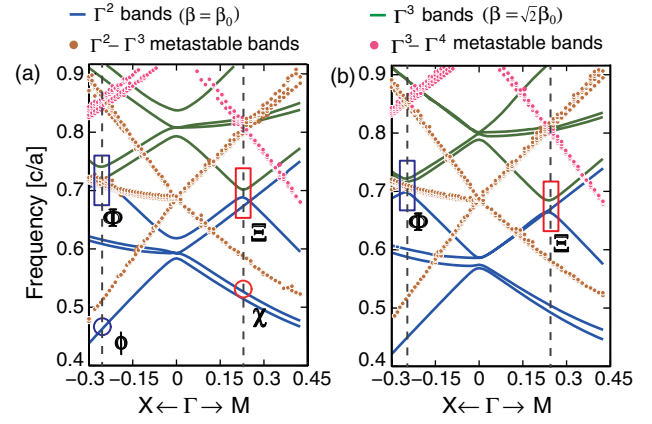
The tunable BICs ϕ [Fig. 4(a)] and χ [Fig. 4(b)] solely occur in TM-like modes.

Thus, the formation of tunable BICs is quite clear: the partial cancellation of the in-plane and the surface coupling ensures rather low radiation ability of the separate closed channels. New accidental symmetry induces strong coupling in via the continuum channels (but still far weaker than the precancellation within single closed channels). Finally, scanning of the wave vector allows achieving the weighted destructive interference between the closed and open channels. The via the continuum coupling also exists for 1D situations [27]. According to the similar phase matching criteria for 2D cases, the 1D case should potentially possess an off-Γ BIC in the vicinity of 0.5 G, which was reported in [9]. Therefore, both fixed BICs [8,19] and tunable BICs [9,20,21] are realizable in 1D and 2D structures.

The off-Γ BICs can also be understood as the interband coupling [28] between the Γ^2 and Γ^3 bands [25]. With infinitely thick PC, the coupling between different Γ orders is forbidden because of orthogonality. However, for PC with finite thickness, the orthogonality is broken, and interband coupling is allowed owing to the indirect via the continuum coupling within near fields. The destructive interference of the via the continuum coupling induces BICs, while the constructive interference forms metastable bands (Fig. 5). Because the mixed metastable modes are not supported by the PC periodicity, they quickly dissipate or couple back to the stable bands, rendering their low Q_r in the entire Brillouin zone.

The discussion of BICs in this Letter focuses on the cancellation of the out-of-plane radiation but neglects the in-plane loss. For a PC slab with a finite area, energy may leak at planar boundaries, causing more loss. The in-plane loss may be negligible for a macroscopic PC slab [19], but it must be considered in realizing a three-dimensional BIC

within a smaller area. Thus, the planar permittivity (i.e., potential) distribution should be addressed to reduce the considerable in-plane loss. For photonics, we believe a damped oscillating planar permittivity envelope is a promising solution, which corresponds to the initial proposal for a quantum system [5].

In this Letter, we provided an analytical perspective for BICs in PC slabs. For separate closed channels, the compensation of in-plane and surface coupling makes TM-like modes easier to trap. By tuning the wave vector, the via the continuum coupling can form weighted destructive interference through new accidental symmetry.

---

[*]pengchao@pku.edu.cn

[1] S. Noda, A. Chutinan, and M. Imada, Nature (London) **407**, 608 (2000).

[2] Y. Akahane, T. Asano, B.-S. Song, and S. Noda, Nature (London) **425**, 944 (2003).

[3] K. Hirose, Y. Liang, Y. Kurosaka, A. Watanabe, T. Sugiyama, and S. Noda, Nat. Photonics **8**, 406 (2014).

[4] B. Min, E. Ostby, V. Sorger, E. Ulin-Avila, L. Yang, X. Zhang, and K. Vahala, Nature (London) **457**, 455 (2009).

[5] J. von Neumann and E. Wigner, Z. Phys. **30**, 465 (1929).

[6] H. Feshbach, Ann. Phys. (N.Y.) **5**, 357 (1958).

[7] H. Friedrich and D. Wintgen, Phys. Rev. A **32**, 3231 (1985).

[8] Y. Plotnik, O. Peleg, F. Dreisow, M. Heinrich, S. Nolte, A. Szameit, and M. Segev, Phys. Rev. Lett. **107**, 183901 (2011).

[9] D. C. Marinica, A. G. Borisov, and S. V. Shabanov, Phys. Rev. Lett. **100**, 183902 (2008).

[10] M. I. Molina, A. E. Miroshnichenko, and Y. S. Kivshar, Phys. Rev. Lett. **108**, 070401 (2012).

[11] E. N. Bulgakov and A. F. Sadreev, Phys. Rev. B **78**, 075105 (2008).

[12] F. Stillinger and D. Herrick, Phys. Rev. A **11**, 446 (1975).

[13] A. Albo, D. Fekete, and G. Bahir, Phys. Rev. B **85**, 115307 (2012).

[14] J. M. Zhang, D. Braak, and M. Kollar, Phys. Rev. Lett. **109**, 116405 (2012).

[15] S. Longhi and G. D. Valle, Sci. Rep. **3**, 2219 (2013).

[16] E. Bulgakov and A. Sadreev, Phys. Rev. B **83**, 235321 (2011).

[17] C. Linton and P. McIver, Wave Motion **45**, 16 (2007).

[18] R. Porter and D. Evans, Wave Motion **43**, 29 (2005).

[19] J. Lee, B. Zhen, S. L. Chua, W. Qiu, J. D. Joannopoulos, M. Soljačić, and O. Shapira, Phys. Rev. Lett. **109**, 067401 (2012).

[20] C. W. Hsu, B. Zhen, J. Lee, S. L. Chua, S. G. Johnson, J. D. Joannopoulos, and M. Soljačić, Nature (London) **499**, 188 (2013).

[21] C. W. Hsu, B. Zhen, S.-L. Chua, S. G. Johnson, J. D. Joannopoulos, and M. Soljačić, Light Sci. Appl. **2**, e84 (2013).

[22] Y. Liang, C. Peng, K. Sakai, S. Iwahashi, and S. Noda, Phys. Rev. B **84**, 195119 (2011).

[23] C. Peng, Y. Liang, K. Sakai, S. Iwahashi, and S. Noda, Phys. Rev. B **86**, 035108 (2012).

[24] Y. Yang, C. Peng, and Z. Li, Opt. Express **21**, 20588 (2013).

[25] S. Iwahashi, Y. Kurosaka, K. Sakai, K. Kitamura, N. Takayama, and S. Noda, Opt. Express **19**, 11963 (2011).

[26] Y. Yamamoto, T. Kamiya, and H. Yanai, IEEE J. Quantum Electron. **14**, 620 (1978).

[27] Y. Yamamoto, T. Kamiya, and H. Yanai, IEEE J. Quantum Electron. **14**, 245 (1978).

[28] J. N. Winn, S. Fan, J. D. Joannopoulos, and E. P. Ippen, Phys. Rev. B **59**, 1551 (1999).